NeuroImage 91 (2014) 169–176

Contents lists available at ScienceDirect

NeuroImage

journal homepage: www.elsevier.com/locate/ynimg

Sleep deprivation reduces the rate of rapid picture processing

Danyang Kong [a], Christopher L. Asplund [a,b], Michael W.L. Chee [a,*]

[a] Center for Cognitive Neuroscience, Neuroscience & Behavioral Disorders Program, Duke-NUS Graduate Medical School, Singapore
[b] Division of Social Sciences (Psychology), Yale-NUS College, Singapore

ARTICLE INFO

Article history:
Accepted 20 January 2014
Available online 25 January 2014

ABSTRACT

Object recognition becomes impaired at faster presentation rates and here we show the neuroanatomical foci of where this might be exacerbated by sleep deprivation (SD). Twenty healthy human participants were asked to detect a target house in serially presented house pictures that appeared at 1–15 images/s. Temporal response profiles relating fMRI signal magnitude to presentation frequency were derived from task-responsive regions. Following SD, the inverted U-shaped response profile within parahippocampal place area was lower and peaked at a slower presentation rate than when participants slept normally. Contrastingly, SD did not shift the relatively monotonic early visual cortex responses. The intraparietal sulci but not the frontal eye fields or medial frontal region, showed similar shifts in temporal response profiles following SD, suggesting differential contribution of areas mediating attention control towards limiting rapid object processing. As nodes of the default mode network (DMN) continued to show monotonically increasing deactivation at higher presentation frequencies even following SD, the observed state modulations of temporal responses likely represent temporal limitations in object processing as opposed to task disengagement.

Introduction

Deficits in visual attention, accompanied by reductions in fronto-parietal and visual extrastriate cortex activation, are among the most robust neurobehavioral changes observed after one-night's sleep deprivation (Chee et al., 2008, 2010; Lim et al., 2007; Tomasi et al., 2009; Tucker et al., 2010). Associated alterations in visual processing include effects on visual short term memory (Chee and Chuah, 2007), peripheral perceptual processing capacity (Kong et al., 2011), distractor suppression (Kong et al., 2012), and tracking moving-objects (Tomasi et al., 2009). Although it is clear that attention facilitates perception (Kastner and Ungerleider, 2000; Reynolds and Chelazzi, 2004), the effect of SD on the rate at which we can process visual information remains unexplored. The visual system processes information with amazing rapidity, such that we can identify a single flashed object appearing for as briefly as 20 ms (Thorpe et al., 1996), a speed unrivaled by most man-made systems (Grill-Spector and Kanwisher, 2005; Thorpe et al., 1996). The associated ability to process serially presented images briefly separated in time is of interest here given the relevance of this faculty in tasks performed by sleep-deprived persons such as threat detection or rapid radiologic diagnosis.

Rapid Serial Visual Presentation (RSVP) sequences of faces and houses have been used to identify loci exhibiting temporal processing limitations within visual cortex. The hierarchical organization of visual cortex whereby neurons in higher visual areas respond to increasingly complex stimulus features or object classes, suggests a progressive loss of sensitivity at higher presentation rates in higher areas like the parahippocampal place area (PPA). Accordingly, temporal limitations in processing involving the PPA and face areas have been demonstrated using fMRI (Gauthier et al., 2012; McKeeff et al., 2007).

We examined how sleep deprivation (SD) affects visual object processing by having participants view serially presented house pictures at different rates. Visual cortex activation can be expected to increase with greater sensory stimulation at higher presentation rates. However, when processing capacity is limited, activation will decline at faster presentation rates, resulting in an inverted u-shaped temporal response profile. We would further expect a lower peak as well as a leftward shift of response profile during SD. Contrastingly, in areas where visual processing is not limited at the presentation frequencies tested, a monotonic increase in activation would be expected. As cognitive models posit a second stage of identification, recognition, and report of visual stimuli beyond perceptual analysis (Chun and Potter, 1995; Marois et al., 2004b), we also studied fronto-parietal areas previously shown to be affected by SD. Finally, we assessed whether 'reduced visual

* Corresponding author at: Centre for Cognitive Neuroscience, Duke-NUS Graduate Medical School, 8 College Rd, #06-18, Singapore 169857, Singapore. Fax: +65 62218625.
E-mail address: michael.chee@duke-nus.edu.sg (M.W.L. Chee).

http://dx.doi.org/10.1016/j.neuroimage.2014.01.037

processing capacity' could have resulted from disrupted task engagement by examining responses in default mode regions to increasing rate of picture presentation.

Materials and methods

Participants

Twenty healthy right-handed participants (mean age 22.95 ± 1.55 years; 7 females) took part in this study. All participants provided informed consent, in compliance with a protocol approved by the National University of Singapore Institutional Review Board. They were selected from respondents to a web-based questionnaire who: (1) were right-handed, (2) had regular sleeping habits, (3) slept no less than 6.5 h/night, (3) were not on any long-term medications, (4) had neither symptoms nor history of sleep disorders, (5) had no history of psychiatric or neurologic disorders, (6) drank less than 3 caffeinated drinks per day and (7) were not of an extreme chronotype as assessed by the Horne–Östberg Morningness–Eveningness questionnaire (Horne and Östberg, 1976), i.e. having a score between 35 and 65. The sleeping pattern of each participant was monitored throughout the entire duration of the study and only those whose actigraphy (Actiwatch, Philips Respironics, USA) data indicated habitual good sleep (i.e., sleeping no later than 12:30 AM and waking no later than 9:00 AM) were recruited following informed consent. All participants indicated that they did not smoke, consume any medication, stimulants, caffeine or alcohol for at least 24 h prior to scanning.

Study procedure

Participants made three visits to the laboratory. The first was a briefing session during which they were informed about the study protocol and requirements. Eligible persons practiced one run of the study task. At the end of this session, they were given a wrist actigraph to wear throughout the study.

Participants were scanned twice, once during rested wakefulness (RW) and once following SD. The order of the scans was counterbalanced across participants, and the sessions were separated by a minimum of one week to minimize residual effects of sleep deprivation on cognition for participants who underwent the SD session first.

RW scans took place at 8:00 AM. Participants arrived at the laboratory at 9:30 PM the night prior to the morning scan and were given a 9-hour sleep opportunity in a dark, quiet, air-conditioned room. For the SD session, participants arrived at the laboratory at 7:00 PM, after staying awake the whole day without napping. They were subsequently monitored in the laboratory. SD scans took place at about 6:00 AM the next day.

The scanning times were deliberately chosen as they represent the typical start time of a regular workday and the time when vigilance hits a nadir after a night of sleep deprivation (Doran et al., 2001; Graw et al., 2004). The effects described here represent a combination of homeostatic and circadian effects on neurobehavioral performance intended to simulate the difference in performance obtained at the start of the work day for a young adult and the effect of having to work through a night shift without sleep. During the SD session, participants were allowed to engage in non-strenuous activities such as reading, watching videos and conversing under artificial lighting of about 200 lux (office level light). Vigorous physical activity prior to the scans was not permitted. Every hour throughout the study night, participants performed a short battery of psychometric tests consisting of the Psychomotor Vigilance Task (Dinges et al., 1997), a Likert-type rating scale (0–10) of motivation, fatigue and mood, and the Karolinska Sleepiness Scale (Åkerstedt and Gillberg, 1990).

Experimental design

The experiment investigated how SD influenced temporal processing limits. Each experimental session (RW or SD) comprised six runs, each of 288 s duration. Prior to each run, participants were asked to memorize two house targets. A short recognition test was administered to ensure that these were remembered prior to scanning.

During each functional imaging run, participants viewed RSVP sequences of gray-scale house images (10° × 10°) that appeared at 1, 2, 4, 6, 8.5 or 15 images/s (monitor frame rate, 60 Hz). Each 8-s trial consisted of a 4-s RSVP sequence and a 4-s fixation period (Fig. 1). Images were presented through MR-compatible LCD goggles (Nordic Neurolab, Bergen, Norway). In addition to these picture-containing sequences were two 'blank' trials that contained only a fixation cross, to vary the inter-trial intervals. The eight trial types were counterbalanced so that each was equally likely to be preceded and followed by every other trial type. In total, there were 26 trials of each presentation frequency. This was to ensure that even in SD where misses might be expected, each trial type contributed at least 20 trials to the model.

Only one target was present in each RSVP sequence. At the end of each sequence, participants were required to report which of these two target houses was presented (2AFC). They were instructed to respond as accurately and as quickly as possible, using their right index and middle fingers via a MR-compatible response box (Current Designs, Philadelphia, USA). An eye camera (Nordic Neurolab, Bergen, Norway) was used to continuously monitor for eyelid closures. Participants were prompted through the intercom system whenever they failed to respond to two consecutive trials. While auditory alarms can arouse, they are absolutely necessary. To mitigate these effects, we limited the range of lapsing allowed of our subjects, effectively compressing the range of detectable effects. Participants who had a 20% non-response rate or greater were eliminated from the study.

Functional localizer

Functional localizer scans were collected in a separate session. These were used to identify the PPA for each individual participant using well-documented procedures (Epstein and Kanwisher, 1998; Kanwisher et al., 1997; Tong et al., 1998). Each session comprised two 328-s runs, each of which consisted of 16 alternating house and face blocks. Twenty house or face images were shown in each block. Images used in the localizer runs had identical dimensions as those used in the main experiment (10° × 10°). Each image appeared for 300 ms followed by 500 ms

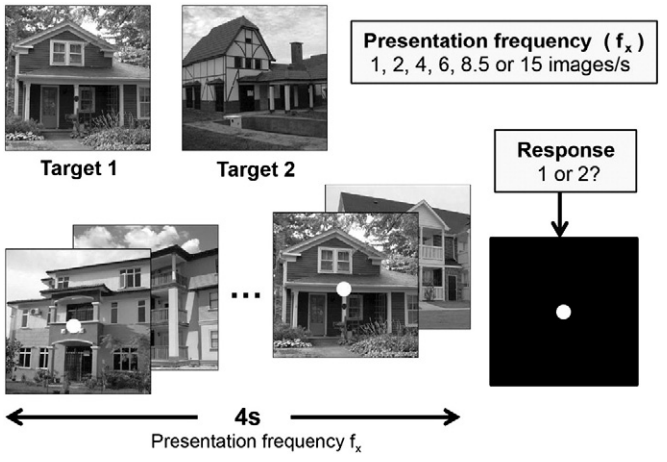

Fig. 1. Schematic of the experimental task. Sequences of house images were presented at six different presentation rates: 1, 2, 4, 6, 8.5 and 15 images/s. At the end of each sequence, participants reported which of the two targets was present.

of fixation. After every four blocks of presentation, a 16-s fixation period followed.

Imaging procedure

Structural and functional images were acquired on a 3-Tesla Tim Trio system (Siemens, Erlangen, Germany) using a 12-channel head coil.

Functional images were collected using a gradient echo-planar imaging sequence with TR 2000 ms, TE 30 ms, FA 75°, FOV 192 × 192 mm and a 64 × 64 matrix. For each functional volume, thirty-six oblique axial slices (3 mm thick with a 0.3 mm inter-slice gap) parallel to the AC-PC line were acquired. High-resolution coplanar T1-weighted anatomical images were also obtained. Finally, a high-resolution anatomical reference image was acquired using an MPRAGE sequence (TR 2300 ms, TI 900 ms, flip angle 9°, BW 240 Hz/pixel, resulting voxel dimensions: 1.0 × 1.0 × 1.0 mm).

Data analysis

The functional images were processed using Brain Voyager QX version 1.10.4 (Brain Innovation, Maastricht, the Netherlands) and custom routines written in MATLAB R2012a (Version 8.0) (Mathworks). After serially inspecting each functional volume for gross intensity fluctuations and movement, the image data was preprocessed using rigid-body motion correction (trilinear and sinc interpolation; corrected relative to first volume after the coplanar image), slice scan time correction, spatial smoothing (4 mm FWHM Gaussian kernel), and temporal high-pass filtering (3 cycles per run). Automatic co-registration of the anatomical and functional images was checked and adjusted manually, after which the images were then transformed into Talairach space.

Imaging data analyzed using a general linear model with 12 main predictors, one for each presentation frequency/condition (1, 2, 4, 6, 8.5 and 15 images/s) in each of the two states. Missed trials were modeled using a separate predictor. Each predictor was created by convolving a boxcar function of 4 s duration, with a canonical double-gamma hemodynamic response function.

To examine the response profile across presentation rates, regions of interest (ROIs) were first defined from the conjunction map of RW and SD activation [(activation in all conditions during RW > RW baseline) ∩ (activation in all conditions during SD > SD baseline)] (Nichols et al., 2005). This map showed task activated areas shared across both states. These ROIs included regions within the fronto-parietal attention network – intraparietal sulcus (IPS), frontal eye field (FEF), and medial frontal gyrus (MeFG) – and regions within the default mode network, including posterior cingulate cortex (PCC) and the inferior parietal lobule (IPL). Cubes of edge 9 mm centered on the peak voxel ($p < 10^{-8}$, uncorrected) around each peak constituted each ROI. The PPA in each hemisphere was individually defined with functional localizer scans (contrast: house > face). The early visual cortex was defined by drawing a cube of edge 9 mm centered on the each calcarine sulcus.

Temporal response profiles were constructed for each participant, region of interest, and state (RW and SD). These profiles showed activation (parameter estimates for each predictor) as a function of image presentation frequency. We hypothesized that humans process rapidly presented pictures less well when sleep deprived compared to when they are well-rested. As the instantiation of our hypothesis hinges on the demonstration of statistically significant leftward shift in the temporal response profiles, we showed this using three approaches.

First, we identified the presentation frequency (1, 2, 4, 6, 8.5 or 15 images/s) at which the highest fMRI activation was observed in a given ROI and for a given participant. This frequency: $f_{i,\ max}$, was determined separately for each state ($f_{i,\ RW\_max}$, $f_{i,\ SD\_max}$). A two-tailed paired *t*-test was used to determine whether presentation frequency differed significantly across RW and SD.

Second, a permutation test was conducted to ascertain the probability that the frequency at which activation peaked differed across the two states by chance. As previously described, we first determined the presentation frequency associated with the maximal activation in each state and for each participant: ($f_{1,\ RW\_max}$, $f_{1,\ SD\_max}$), …, ($f_{n,\ RW\_max}$, $f_{n,\ SD\_max}$), where n = number of participants. The t-value of the paired *t*-test comparing values in this array specified t_{obs}.

Permutations were generated by swapping $f_{i,\ RW\_max}$ and $f_{i,\ SD\_max}$ across the 20 participants in a random manner while ensuring that a given permutation was not repeated. A paired *t*-test was carried out for each permutation to yield t_{perm} which was then compared with the observed data (t_{obs}). The p-value of the permutation test was defined as: Count ($t_{perm} \geq t_{obs}$) / k, where k is the number of permutations tested. We tested 5000, 10,000 and 20,000 permutations.

A quadratic function was used to fit the response profiles obtained for each subject and ROI. Presentation rates were natural log transformed in order to allow estimation of the peak/trough of the temporal response profile in each ROI. Each fit was bounded by the minimum and maximum presentation rates used in the study. The state-related shift in the function's peak was compared in each region using a paired *t*-test.

To compare the curvilinearity of the temporal response profile in each ROI, group level fMRI responses across the six different presentation frequencies in each ROI were modeled by both linear and quadratic functions. Corrected Akaike information criterion (AIC_c) values were calculated (Akaike, 1974) and $\Delta AIC_c = AIC_c - AIC_{c\_min}$ was used to compare the different models (Burnham and Anderson, 2002).

Results

Behavioral results

In RW, participants had a non-response rate 0.5% of all trials, while in SD this increased to an average of 8%. Across the 20 participants and both RW and SD sessions, we only encountered 7 cases of participants who failed to respond to two consecutive trials and required prompting.

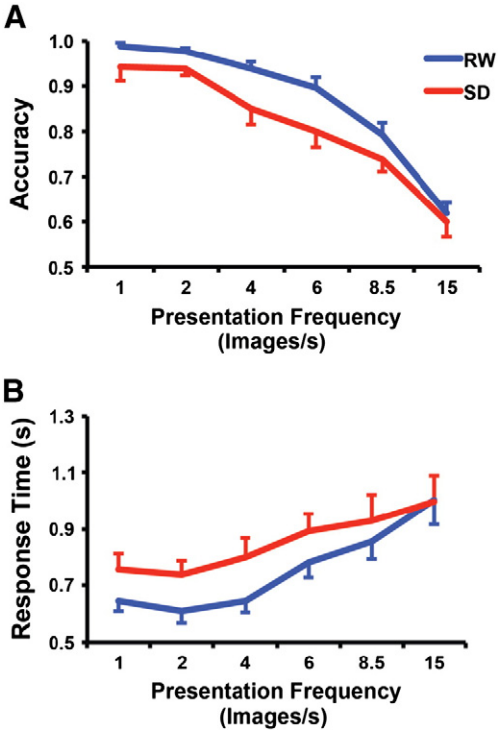

Fig. 2. Behavioral results. (A) Performance was impaired both during sleep deprivation and at higher presentation frequencies. (B) Significant state by rate interaction was present for response time.

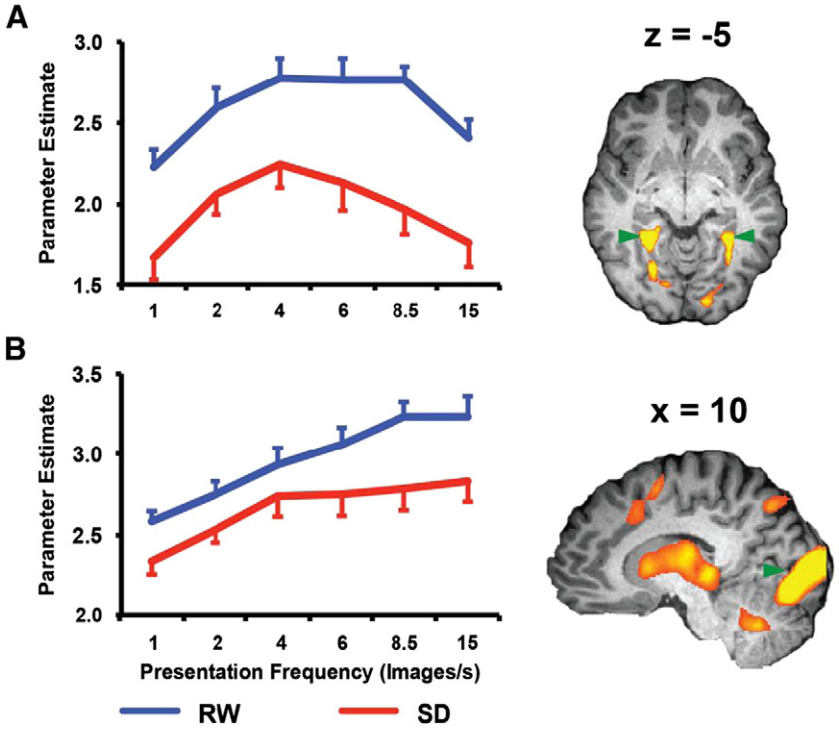

Fig. 3. (A) Temporal response profiles across state in PPA. Parameter estimates are in arbitrary units. Group activation map showing the PPA, thresholded at $p < 0.000005$, uncorrected (average peak Talairach co-ordinates, left PPA: −30, −48, −5; right PPA: 25, −46, −6). (B) Temporal response profiles across state in the early visual cortex. Group activation map showing early visual cortex, thresholded at $p < 0.000005$, uncorrected (average peak Talairach co-ordinates, left: −12, −91, −2, right: 9, −91, 4). Note that the y-axis scale has been cropped to optimally display relevant activation magnitude values in the PPA and early visual cortex.

There were main effects of state ($F_{1, 19} = 21.37$; $p < 0.0001$) and presentation frequency ($F_{5, 95} = 94.71$; $p < 0.0001$; Fig. 2A) on target detection accuracy. Accuracy was lower following sleep deprivation and with higher presentation rates, reaching near-chance performance around 15 images/s. There was a significant state by frequency interaction on response time ($F_{5, 95} = 5.27$; $p < 0.001$) in addition to main effects of state ($F_{1, 19} = 8.05$; $p < 0.05$; slower in SD) and presentation frequency ($F_{5, 95} = 18.82$; $p < 0.0001$; slower with higher presentation rates; Fig. 2B).

Imaging findings

There were main effects of presentation frequency ($F_{5, 95} = 34.64$; $p < 0.0001$) and state on PPA activation ($F_{1, 19} = 20.69$; $p < 0.0001$; lower during SD). There was also a significant state by rate interaction in the PPA ($F_{5, 95} = 2.39$; $p < 0.05$), indicating that PPA temporal response profiles differed across states (Fig. 3A).

Without assuming the form of the temporal response function, the average presentation frequency at which the highest fMRI activation was observed in PPA was 5.83 images/s during RW and 4.15 images/s during SD ($t = 3.84$, $p = 0.001$; Table 1).

Using a quadratic fit, the presentation frequency at which PPA activation peaked was 5.1 images/s in RW and 3.8 images/s following SD ($t_{19} = 2.91$, $p < 0.01$). Finally, permutation tests also showed that there was a significant leftward shift in the temporal response profile across states; corresponding p values for tests with 5000, 10,000 and 20,000 permutations were 0.0068, 0.0051 and 0.0038.

In contrast to responses in the PPA, early visual areas showed an increase in activation with increasing presentation frequency within the range tested ($F_{5, 95} = 31.36$; $p < 0.0001$). SD also attenuated activity in early visual cortex ($F_{1, 19} = 10.13$; $p < 0.01$). The shape of the temporal response function was monotonic rather than quadratic (Fig. 3B; Table 2).

A three-way repeated measures ANOVA with brain region (PPA versus early visual areas), state and frequency as factors found significant two-way interactions – region by state ($F_{1, 19} = 22.67$; $p < 0.0001$), area by frequency ($F_{5, 95} = 28.88$; $p < 0.0001$) and state by frequency ($F_{5, 95} = 3.28$; $p < 0.001$) – indicating that activation in PPA and early visual cortex was differentially modulated by state and by presentation frequency.

The fMRI temporal response profile in the IPS following SD resembled the inverted U-shaped function found in PPA (Fig. 4A). There was a significant state by presentation frequency interaction ($F_{5, 95} = 2.29$; $p < 0.05$) in addition to main effects of frequency ($F_{5, 95} = 6.22$; $p < 0.0001$) and state ($F_{1, 19} = 9.61$; $p < 0.01$). Similar to PPA, activation in IPS peaked at a significantly slower rate during SD ($t_{19} = 2.70$; $p < 0.05$; Fig. 4A; Table 1). Permutation testing was congruent with this finding; corresponding p values for tests with 5000, 10,000 and 20,000 permutations were 0.045, 0.038 and 0.034. It is possible that the temporal response profile in RW was not quadratic because the 'u-shape' of the function was beyond the tested range of frequencies.

Activation in FEF showed significant main effect of state ($F_{1, 19} = 3.33$; $p < 0.05$) and presentation frequency ($F_{5, 95} = 6.13$; $p < 0.0001$). In MeFG, there was a main effect of presentation frequency ($F_{5, 95}$

Table 1
Paired t-tests comparing peaks/troughs of the temporal response profiles obtained from different brain regions. Note the peak frequencies here were obtained by assessing the frequency at which maximum activation was observed for each individual and for each state and region — these maxima were not derived from curve fitting c.f. main text.

	Peak/trough		Paired *t*-test	
	RW (Images/s)	SD (Images/s)	t-statistic (df = 19)	p value
Early visual cortex	11.95	10.28	1.57	n.s.
PPA	5.83	4.15	3.84	$p = 0.001$
IPS	7.25	5.35	2.70	$p < 0.05$
FEF	8.33	6.90	0.94	n.s.
MeFG	9.23	8.68	0.49	n.s.
PCC	11.05	10.2	0.53	n.s.
IPL	9.93	9.35	0.38	n.s.

Table 2
We calculated Akaike information criterion (AIC_c) associated with linear and quadratic model fits of temporal response profiles obtained from 7 brain regions: parahippocampal place area (PPA), intraparietal sulcus (IPS), frontal eye field (FEF), and medial frontal gyrus (MeFG), posterior cingulate cortex (PCC) and the inferior parietal lobule (IPL). AIC_c differences, ΔAIC_c, were computed to ascertain if linear or quadratic models better fit the data. If $\Delta AIC_c \leq 2$, the quadratic and linear models have comparable explanatory power; if the values of ($AIC_{c\_L} - AIC_{c\_Q}$) lie between the range of 4–7, a quadratic model is considered superior; and beyond this, we can safely rule out the linear model as a plausible fit for the data compared to the quadratic model (Burnham and Anderson, 2002).

	RW			SD		
	AIC_{c_L}	AIC_{c_Q}	ΔAIC_c	AIC_{c_L}	AIC_{c_Q}	ΔAIC_c
Early visual cortex	76.8	78.6	1.8	143.0	143.5	0.5
PPA	163.0	144.2	18.8*	243.4	234.1	9.3*
IPS	180.5	180.0	0.5	235.4	229.5	5.9*
FEF	145.7	147.7	2.0	192.1	192.3	0.2
MeFG	140.7	140.8	0.1	155.2	157.3	2.1
PCC	132.0	133.8	1.8	145.9	147.0	1.1
IPL	169.3	168.7	0.6	185.9	187.6	1.7

$= 11.54$; $p < 0.0001$) and a significant state by frequency interaction ($F_{5, 95} = 4.71$; $p < 0.001$). However, in contrast to IPS, FEF and MeFG did not show a significant drop in activation at the highest presentation frequencies tested here, even following sleep deprivation (Figs. 4B and C; Table 1).

To test whether the temporal profiles of PPA, IPS, FEF and MeFG were better characterized by linear or quadratic functions, we calculated group-level AICs for these two models and compared delta AICs (Table 2). Quadratic models described the temporal response profiles significantly better than linear models in PPA in both states and IPS following SD, whereas the AIC values for both models were comparable in FEF and MeFG. Thus, there appeared to be differences in the curvilinearity of the temporal response profiles, with quadratic profiles in posterior regions and linear ones anteriorly (from PPA, IPS, FEF to MeFG).

Posterior cingulate cortex (PCC) and inferior parietal lobule (IPL), nodes of the default mode network (DMN), showed task-induced deactivation that was modulated by presentation frequency (Fig. 5). Across both states, these regions showed monotonic increases in deactivation with increasing presentation frequency (PCC: $F_{5, 95} = 16.23$, $p < 0.0001$; IPL: $F_{5, 95} = 17.68$, $p < 0.0001$; Table 1). There was a significant main effect of state in both PPC and IPL regions (PCC: $F_{1, 19} = 5.69$, $p < 0.05$; IPL: $F_{1, 19} = 8.37$, $p = 0.01$).

Discussion

Rapid serial visual presentation of house pictures allowed us to identify the neural correlates of reduced object processing speed following sleep deprivation. SD had dissociable effects on the temporal response profiles elicited from PPA and early visual cortex, with the PPA response peaking at a lower rate following SD. A similar shift in temporal response was observed in the IPS, suggesting that it may serve as or be affected by a bottleneck of rapid visual object processing. A main effect of state was present for task-related deactivation, but its monotonic change with increasing presentation rate suggests that participants remained engaged in the task even when sleep deprived.

Sleep deprivation slows rapid processing of complex images in higher visual cortex

SD effects on visual processing speed likely result in reduced information processing capacity. The simplest method of assessing the former is to determine the critical flicker fusion frequency (CFF), the maximal rate at which consecutive flashes of light can be discerned as separate (Landis, 1953). Variations of this technique have been used to assay the effects of drugs in psychopharmacology applications. However, unlike RSVP picture sequences, CFF does not distinguish between the contributions of early and higher visual cortex to processing speed. This may be why testing critical fusion frequency using elementary stimuli has not shown consistent effects during total sleep deprivation (Lee et al., 2002) or restricted sleep (Leonard et al., 1998).

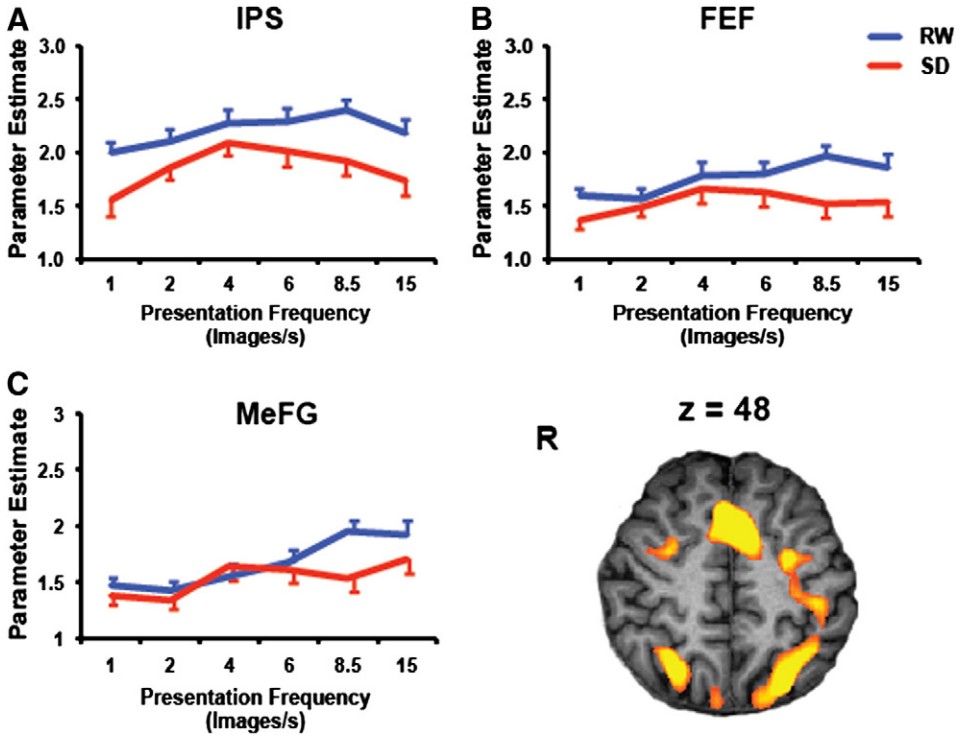

Fig. 4. Temporal response profiles across state in IPS, FEF and MeFG. Group activation map shows the IPS, FEF and MeFG, thresholded at $p < 0.000005$, uncorrected (average peak Talairach co-ordinates, left IPS: −29, −57, 45; right IPS: 26, −57, 44; left FEF: −29, −6, 49; right FEF: 29, −3, 50; MeFG: −3, 7, 48).

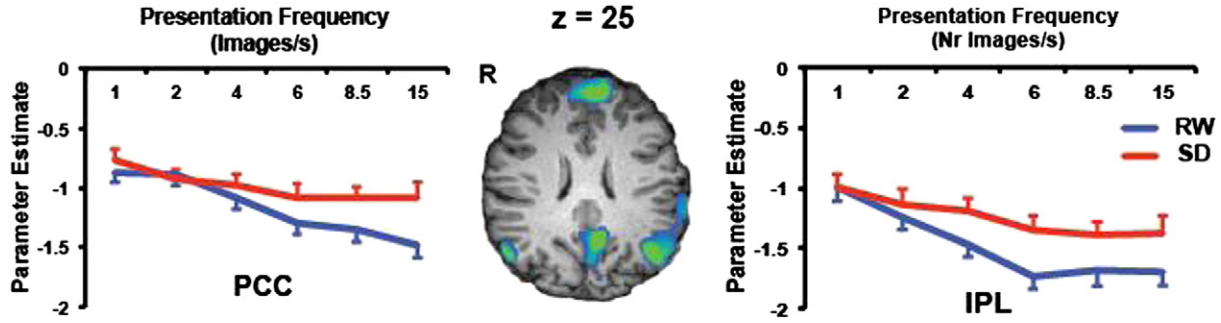

Fig. 5. Temporal response profiles in regions showing task-induced deactivation (averaged peak Talairach co-ordinates, right IPL: 44, −64, 25; left IPL: −44, −63, 24; PCC: −6, −50, 27). Group map thresholded at $p < 0.000005$, uncorrected.

Early visual cortex rapidly processes low-level features (Boynton et al., 1999; Grill-Spector and Malach, 2004; Ress and Heeger, 2003). Consequently, even with short-duration stimuli presented at high frequencies, early visual cortex can respond with increasing fMRI activation (Grill-Spector et al., 2000; McKeeff et al., 2007). As one traverses the visual processing hierarchy, the complexity of visual representations increases (Grill-Spector, 2003), corresponding to greater dependencies on earlier visual areas and longer processing times (Einhauser et al., 2007; Todd et al., 2011). For example, the PPA gradually integrates information relayed from the earlier visual regions to process complex features implicit to houses (Einhauser et al., 2007; Epstein and Kanwisher, 1998; Todd et al., 2011). As such, PPA activation increases when more processing time is provided but this reaches an asymptote at around 120 ms (Grill-Spector et al., 2000).

Unlike early visual cortex, which is highly responsive to target durations and transient signals such as blinks (Gawne and Martin, 2000), higher visual areas are more sensitive to the stimulus onset asynchrony (SOA) between a complex target and its trailing distractor (Grill-Spector et al., 2000). This sensitivity may reflect the buffering of perceptual information in reverberatory neural circuits (Tallon-Baudry et al., 2001), that supports additional information processing in higher visual areas. Indeed, sufficiently long SOAs allow the integration of visual information to continue after the disappearance of a briefly presented stimulus (Gauthier et al., 2012). Furthermore, if stimulus duration is varied but the SOA is held constant at a length sufficient for such integration to occur, firing patterns in monkey superior temporal sulcus (STS) remain indistinguishable across different presentation durations (Keysers et al., 2005).

Contrastingly, if a new stimulus or a backward mask occurs before the threshold stimulus duration, information processing is disrupted, attenuating the associated neural response as well as impairing object recognition (Ansorge et al., 2007; Gauthier et al., 2012; Keysers et al., 2005). In the present experiment, we posit that fMRI activation declines when the duration between successive stimuli drops below the minimum required for successful processing and integration.

It follows that relative to early visual cortex, higher visual areas like the PPA may be more vulnerable to state-induced alterations in brain function. As such, the current findings extend prior results concerning the dissociated effects of sleep deprivation on early and higher visual areas (Chee and Chuah, 2007; Chee et al., 2010; Kong et al., 2011, 2012). Critically, in the present work, PPA activation was modulated by the interaction of state and presentation frequency, instead of merely being attenuated across all conditions as was observed with incrementing visual short-term memory load during SD (Chee and Chuah, 2007).

A related notion arising from the present study relates to 'local sleep' models of behavior in sleep-deprived participants, where stochastically impaired behavior has been attributed to cortical columns spontaneously entering the 'off' state (Pigarev et al., 1997; Vyazovskiy et al., 2011). These models have been proposed to explain behavioral lapses that involve 'all or none' effects on behavior (Vyazovskiy et al., 2011; Wee et al., 2013). However, another consequence of random neurons entering the 'off' state is degraded quality of information processing. This may occur when the functional redundancy of neuronal activation is compromised in SD, thereby increasing the probability that sensory information fails to be transmitted (Chee et al., 2011). Here, the reduced temporal sensitivity of the PPA to high presentation frequencies contrasts with the relative preservation of responses at all frequencies in the early visual cortex, suggesting that 'quality' of information processing between these regions may be affected during the sleep deprived state.

Visual processing limitations beyond the visual cortex

As fronto-parietal regions mediating attentional control show increasing activity commensurate with task demands (Marois et al., 2004a), one might expect IPS and FEF to show monotonically increasing or saturating activation at higher presentation frequencies. Against this prediction, the IPS exhibited a response function peak that shifted to a lower presentation rate during SD. This result is consistent with the proposal that in addition to its role in top-down control of visual attention activity in fronto-parietal regions is modulated by bottom-up visual processing (Sato et al., 2003). Indeed, a combination of bottom-up perceptual information with top-down goals and contexts are required to specify an object of interest (Corbetta and Shulman, 2002).

It has also been proposed that visual perception occurs in two stages, a first stage involving perceptual analysis and a second stage requiring identification and recognition of visual events (Chun and Potter, 1995; Marois et al., 2004b). Recent studies indicate that identification and recognition of objects involve regions other than visual cortex, particularly those traditionally imputed with the control of attention. For example, the inferior IPS is recruited during a coarse object individuation stage while the superior IPS is engaged in object identification that requires fine-resolution target information (Xu, 2009; Xu and Chun, 2009). Electrophysiological recordings show independent parietal cortex contributions to nonspatial functions such as visual categorization and the coding of abstract category signals important for object recognition (Rishel et al., 2013).

Accordingly, the present finding of altered temporal response profiles in the IPS is consistent with the existence of visual processing bottlenecks at loci beyond the visual cortex (Marois et al., 2004b). Interestingly, the extent to which activation associated with increasing presentation speed departs from linear was most pronounced in the PPA followed by the IPS but sparing FEF and MeFG. This might reflect a hierarchical organization of perceptual processing and top-down target specification characteristics involving these different areas.

Relative integrity of task engagement

When inferring processing limitations from parametric designs of increasing load, a perennial concern is whether attenuated activation under conditions of higher perceptual or cognitive load reflects capacity constraints of interest, or merely volunteer disengagement. In the current dataset, two findings make the latter account improbable. First, as alluded to earlier, the shift in PPA's temporal response profile cannot be explained by a simple loss of interest in the task during sleep deprivation, as the function's overall shape was virtually identical in the same participants when well rested. Second, the pattern of signal changes in the default mode network (DMN) suggests continued task engagement across presentation rates, even in the sleep-deprived state.

As components of the DMN, the posterior cingulate cortex/precuneus (PCC) and bilateral inferior parietal lobule (IPL) are deactivated during externally-oriented, attention-demanding tasks (Raichle et al., 2001; Shulman et al., 1997). The magnitude of such DMN deactivation reflects the allocation of resources to fulfill task demands (McKiernan et al., 2003; Takeuchi et al., 2011). Contrastingly, mind-wandering and internally-directed cognition have been associated with DMN engagement (Mason et al., 2007). Here, task-induced deactivation in the PCC and bilateral IPL monotonically tracked increasing presentation rates, suggesting relatively preserved task engagement even in SD. Hence, although the overall deactivation in DMN activity was reduced following SD, there was a progressive increase in deactivation with increasing presentation frequency. This makes it less likely that the participants 'tuned out' from the more difficult, faster presentation frequencies. This could give rise to a leftward shift in the temporal response profiles in the PPA that is unrelated to reduced ability to rapidly process visual information.

Conclusion

Visual processing speed declines in the sleep-deprived state. Information processing bottlenecks occur in higher 'visual' areas that process objects and may involve 'attention' regions as well. These changes in visual processing are not readily attributable to task disengagement and likely reflect the overall reduction in the number of functional neural circuits that can be recruited in the sleep-deprived state.

Acknowledgments

Chee Wei Yan, Vinod Shanmugam, Ling Aiqing, Tiffany Chia Ting Yu, Deepti Mulick, Siti Yaakub, Loh Kep Kee, Natalie Wee, Cher Wei Shan and Annalissa Tiu Munoz contributed to the data collection. This work was supported by a grant awarded to Dr. Michael Chee from the National Medical Research Council Singapore (STaR/0004/2008).

Conflict of interest

The authors declare no competing financial interests.

References

Akaike, H., 1974. New look at statistical-model identification. IEEE Trans. Autom. Control. Acta 19, 716–723.
Åkerstedt, T., Gillberg, M., 1990. Subjective and objective sleepiness in the active individual. Int. J. Neurosci. 52, 29–37.
Ansorge, U., Breitmeyer, B.G., Becker, S.I., 2007. Comparing sensitivity across different processing measures under metacontrast masking conditions. Vis. Res. 47, 3335–3349.
Boynton, G.M., Demb, J.B., Glover, G.H., Heeger, D.J., 1999. Neuronal basis of contrast discrimination. Vis. Res. 39, 257–269.
Burnham, K.P., Anderson, D.R., 2002. Model selection and multimodel inference: a practical information — theoretic approach. Springer-Verlag, New York.
Chee, M.W.L., Chuah, Y.M.L., 2007. Functional neuroimaging and behavioral correlates of capacity decline in visual short-term memory after sleep deprivation. Proc. Natl. Acad. Sci. U. S. A. 104, 9487–9492.
Chee, M.W.L., Tan, J.C., Zheng, H., Parimal, S., Weissman, D.H., Zagorodnov, V., Dinges, D.F., 2008. Lapsing during sleep deprivation is associated with distributed changes in brain activation. J. Neurosci. 28, 5519–5528.
Chee, M.W.L., Tan, J.C., Parimal, S., Zagorodnov, V., 2010. Sleep deprivation and its effects on object-selective attention. NeuroImage 49, 1903–1910.
Chee, M.W.L., Goh, C.S.F., Namburi, P., Parimal, S., Seidl, K.N., Kastner, S., 2011. Effects of sleep deprivation on cortical activation during directed attention in the absence and presence of visual stimuli. NeuroImage 58, 595–604.
Chun, M.M., Potter, M.C., 1995. A two-stage model for multiple target detection in rapid serial visual presentation. J. Exp. Psychol. Hum. Percept. 21, 109–127.
Corbetta, M., Shulman, G.L., 2002. Control of goal-directed and stimulus-driven attention in the brain. Nat. Rev. Neurosci. 3, 201–215.
Dinges, D.F., Pack, F., Williams, K., Gillen, K.A., Powell, J.W., Ott, G.E., Aptowicz, C., Pack, A.I., 1997. Cumulative sleepiness, mood disturbance and psychomotor vigilance performance decrements during a week of sleep restricted to 4–5 hours per night. Sleep 20, 267–277.
Doran, S.M., Van Dongen, H.P., Dinges, D.F., 2001. Sustained attention performance during sleep deprivation: evidence of state instability. Arch. Ital. Biol. 139, 253–267.
Einhauser, W., Koch, C., Makeig, S., 2007. The duration of the attentional blink in natural scenes depends on stimulus category. Vis. Res. 47, 597–607.
Epstein, R.A., Kanwisher, N., 1998. A cortical representation of the local visual environment. Nature 392, 598–601.
Gauthier, B., Eger, E., Hesselmann, G., Giraud, A.L., Kleinschmidt, A., 2012. Temporal tuning properties along the human ventral visual stream. J. Neurosci. 32, 14433–14441.
Gawne, T.J., Martin, J.M., 2000. Activity of primate V1 cortical neurons during blinks. J. Neurophysiol. 84, 2691–2694.
Graw, P., Krauchi, K., Knoblauch, V., Wirz-Justice, A., Cajochen, C., 2004. Circadian and wake-dependent modulation of fastest and slowest reaction times during the psychomotor vigilance task. Physiol. Behav. 80, 695–701.
Grill-Spector, K., 2003. The neural basis of object perception. Curr. Opinion Neurobiol. 13, 159–166.
Grill-Spector, K., Kanwisher, N., 2005. Visual recognition: as soon as you know it is there, you know what it is. Psychol. Sci. 16, 152–160.
Grill-Spector, K., Malach, R., 2004. The human visual cortex. Ann. Rev. Neurosci. 27, 649–677.
Grill-Spector, K., Kushnir, T., Hendler, T., Malach, R., 2000. The dynamics of object-selective activation correlate with recognition performance in humans. Nat. Neurosci. 3, 837–843.
Horne, J.A., Östberg, O., 1976. Self-assessment questionnaire to determine morningness-eveningness in human circadian rhythms. Int. J. Chronobiol. 4, 97–110.
Kanwisher, N., McDermott, J., Chun, M.M., 1997. The fusiform face area: a module in human extrastriate cortex specialized for face perception. J. Neurosci. 17, 4302–4311.
Kastner, S., Ungerleider, L.G., 2000. Mechanisms of visual attention in the human cortex. Annu. Rev. Neurosci. 23, 315–341.
Keysers, C., Xiao, D.K., Foldiak, P., Perrett, D.I., 2005. Out of sight but not out of mind: the neurophysiology of iconic memory in the superior temporal sulcus. Cogn. Neuropsychiatry 22, 316–332.
Kong, D., Soon, C.S., Chee, M.W.L., 2011. Reduced visual processing capacity in sleep deprived persons. NeuroImage 55, 629–634.
Kong, D., Soon, C.S., Chee, M.W.L., 2012. Functional imaging correlates of impaired distractor suppression following sleep deprivation. NeuroImage 61, 50–55.
Landis, C., 1953. An annotated bibliography of flicker fusion phenomena covering the period 1740–1952. Armed Forces-National Research Council, Vision Committee Secretariat, University of Michigan, Ann Arbor, Michigan.
Lee, H.J., Yang, J.W., Lee, B.H., Ham, B.J., 2002. Effects of total sleep deprivation on visual discrimination. Sleep Med. Psychophysiol. 9, 122–126.
Leonard, C., Fanning, N., Attwood, J., Buckley, M., 1998. The effect of fatigue, sleep deprivation and onerous working hours on the physical and mental wellbeing of pre-registration house officers. Ir. J. Med. Sci. 167, 22–25.
Lim, J., Choo, W.C., Chee, M.W.L., 2007. Reproducibility of changes in behaviour and fMRI activation associated with sleep deprivation in a working memory task. Sleep 30, 61–70.
Marois, R., Chun, M.M., Gore, J.C., 2004a. A common parieto-frontal network is recruited under both low visibility and high perceptual interference conditions. J. Neurophysiol. 92, 2985–2992.
Marois, R., Yi, D.J., Chun, M.M., 2004b. The neural fate of consciously perceived and missed events in the attentional blink. Neuron 41, 465–472.
Mason, M.F., Norton, M.I., Van Horn, J.D., Wegner, D.M., Grafton, S.T., Macrae, C.N., 2007. Wandering minds: the default network and stimulus-independent thought. Science 315, 393–395.
McKeeff, T.J., Remus, D.A., Tong, F., 2007. Temporal limitations in object processing across the human ventral visual pathway. J. Neurophysiol. 98, 382–393.
McKiernan, K.A., Kaufman, J.N., Kucera-Thompson, J., Binder, J.R., 2003. A parametric manipulation of factors affecting task-induced deactivation in functional neuroimaging. J. Cogn. Neurosci. 15, 394–408.
Nichols, T., Brett, M., Andersson, J., Wager, T., Poline, J.B., 2005. Valid conjunction inference with the minimum statistic. NeuroImage 25, 653–660.
Pigarev, I.N., Nothdurft, H.C., Kastner, S., 1997. Evidence for asynchronous development of sleep in cortical areas. Neuroreport 8, 2557–2560.
Raichle, M.E., MacLeod, A.M., Snyder, A.Z., Powers, W.J., Gusnard, D.A., Shulman, G.L., 2001. A default mode of brain function. Proc. Natl. Acad. Sci. U. S. A. 98, 676–682.
Ress, D., Heeger, D.J., 2003. Neuronal correlates of perception in early visual cortex. Nat. Neurosci. 6, 414–420.
Reynolds, J.H., Chelazzi, L., 2004. Attentional modulation of visual processing. Annu. Rev. Neurosci. 27, 611–647.
Rishel, C.A., Huang, G., Freedman, D.J., 2013. Independent category and spatial encoding in parietal cortex. Neuron 77, 969–979.

Sato, T.R., Watanabe, K., Thompson, K.G., Schall, J.D., 2003. Effect of target-distractor similarity on FEF visual selection in the absence of the target. Exp. Brain Res. 151, 356–363.
Shulman, G.L., Corbetta, M., Buckner, R.L., Fiez, J.A., Miezin, F.M., Raichle, M.E., Petersen, S.E., 1997. Common blood flow changes across visual tasks: II Increases in subcortical structures and cerebellum but not in nonvisual cortex. J. Cogn. Neurosci. 9, 624–647.
Takeuchi, H., Taki, Y., Hashizume, H., Sassa, Y., Nagase, T., Nouchi, R., Kawashima, R., 2011. Failing to deactivate: the association between brain activity during a working memory task and creativity. NeuroImage 55, 681–687.
Tallon-Baudry, C., Bertrand, O., Fischer, C., 2001. Oscillatory synchrony between human extrastriate areas during visual short-term memory maintenance. J. Neurosci. 21, RC177.
Thorpe, S., Fize, D., Marlot, C., 1996. Speed of processing in the human visual system. Nature 381, 520–522.
Todd, J.J., Han, S.W., Harrison, S., Marois, R., 2011. The neural correlates of visual working memory encoding: a time-resolved fMRI study. Neuropsychologia 49, 1527–1536.
Tomasi, D., Wang, R.L., Telang, F., Boronikolas, V., Jayne, M.C., Wang, G.J., Fowler, J.S., Volkow, N.D., 2009. Impairment of attentional networks after 1 night of sleep deprivation. Cereb. Cortex 19, 233–240.
Tong, F., Nakayama, K., Vaughan, J., Kanwisher, N., 1998. Binocular rivalry and visual awareness in human extrastriate cortex. Neuron 21, 753–759.
Tucker, A.M., Whitney, P., Belenky, G., Hinson, J.M., Van Dongen, H.P., 2010. Effects of sleep deprivation on dissociated components of executive functioning. Sleep 33, 47–57.
Vyazovskiy, V.V., Olcese, U., Hanlon, E.C., Nir, Y., Cirelli, C., Tononi, G., 2011. Local sleep in awake rats. Nature 472, 443–447.
Wee, N., Asplund, C., Chee, M.W.L., 2013. Sleep deprivation accelerates delay-related loss of visual short-term memories without affecting precision. Sleep 36 (6), 849–856.
Xu, Y., 2009. Distinctive neural mechanisms supporting visual object individuation and identification. J. Cogn. Neurosci. 21, 511–518.
Xu, Y., Chun, M.M., 2009. Selecting and perceiving multiple visual objects. Trends Cogn. Sci. 13, 167–174.